World Academy of Science, Engineering and Technology
International Journal of Mechanical and Mechatronics Engineering
Vol:6, No:11, 2012

PIV Investigation into the Evolution of Vortical Structures in the Zero Pressure Gradient Boundary Layer

Ishtiaq A. Chaudhry, and Zia R. Tahir

***Abstract*—**Experimental investigation has been carried out towards understanding the complex fluid dynamics involved in the interaction of vortical structures with zero pressure gradient boundary layer. A laminar boundary layer is produced on the flat plate placed in the water flume and the synthetic jet actuator is deployed on top of the plate at a definite distance from the leading edge. The synthetic jet actuator has been designed in such a way that the to and fro motion of the diaphragm is maneuvered at will by varying the operating parameters to produce the typical streamwise vortical structures namely hairpin and tilted vortices. PIV measurements are made on the streamwise plane normal to the plate to evaluate their interaction with the near wall fluid.

***Keywords*—**Boundary layer, synthetic jet actuator, flow separation control, vortical structures.

I. Introduction

IT has been long since the research work has been directed towards exploring the potency of implementing the SJA for delaying flow separation on the aeroplane wing. The design of the actuator is such that without adding a robust part to the wing structure it offers a good mean to utilise the same ambient fluid to synthesize a jet which eventually interacts with the boundary layer to produce stream wise vortical structures. Furthermore the operation is simple in that a range of operating parameters are available to operate the SJA at will to produce a large scale vortical structures at varying free stream conditions.

Though most of the previous work both experimental and numerical simulation [1]-[3], [5], [7] deal with the evolution and development of the vortices in the boundary layer yet much work needs to be directed towards gaining improved understanding of the mechanism involved in the formation and evolution of vortical structures and their eventual interaction with the near wall fluid. Furthermore the reason to direct more experimental work into defining more strict SJA operating parameters to produce similar stream wise vortices under similar free steam conditions as in most of the previous work such parameters are varying widely under similar geometrical and operational settings.

Ishtiaq Ahmed Chaudhry is with the Mechanical Engineering Department, University of Engineering and Technology Lahore, Pakistan currently doing PhD from School of Mechanical Aerospace and Civil Engineering, University of Manchester, UK (corresponding author: e-mail: ishtiaq.ahmed@manchester.ac.uk).

Zia R. Tahir is with the School of Mechanical Aerospace and Civil Engineering, University of Manchester, UK.

II. Experimental Facility

The PIV system used in this work is a commercial system from TSI consisting of Nd:YAG pulse laser (with a maximum power of 135 mJ, repetition rate up to 15Hz and the laser pulse width 3~5 ns), a synchronizer and a power view Plus 4MP CCD camera with a maximum available resolution of 2048×2048 pixels, 12-bit intensity dynamic range and a frame rate up to 16 per second. Nikon high standard micro AF 28mm, 60mm and 105mm focal length lenses were also available to make use of. The camera is positioned such that it faces the laser light plane from the front side as shown in Fig. 1. The suitable laser light sheet with desired thickness and width is formed using a combination of cylindrical and spherical lenses and was directed to the required area on the test plate by using a 50mm thick laser mirror mounted at 45° on a support.

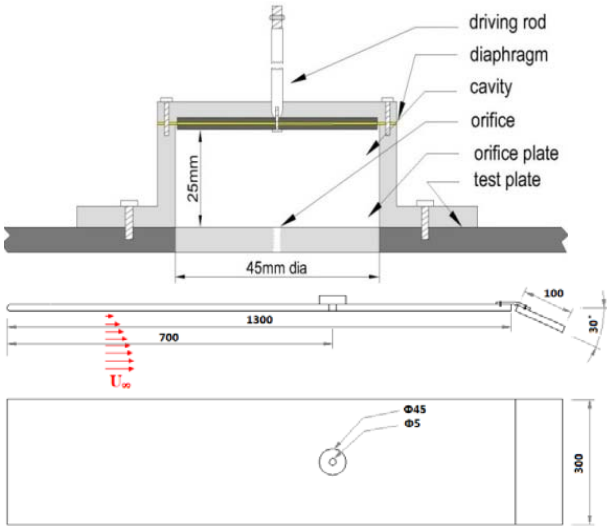

Fig. 1 Schematic of actuator and test plate

III. Results and Discussion

A. Test Conditions

A single circular jet is synthesized from a single orifice placed normal to the surface and issued into cross flow boundary layer with zero pressure gradient attached flow on the flat plate. The SJA operating conditions are summarized in Table II and the geometrical dimensions are same as used in [4]. All the PIV measurements are taken in accordance to the movement and relative position of the piston with respect to maximum/minimum cavity volume that is the start of the cycle

(t/T=0). For phase average measurement at each given position the piston's location is phase locked with the camera to take a shot for that particular phase of the cycle. The cycle starts corresponding to onset of blowing stroke from t/T=0 with the diaphragm located at the farthest position from the orifice that is the maximum volume of the cavity and the blowing stroke completes at t/T=0.50 when the diaphragm is located nearest to the orifice making the cavity volume minimum. The sinusoidal movement of the diaphragm gives the maximum possible jet velocity when the diaphragm is at its neutral position that is t/T=0.25 and the cycle starts/completes when the diaphragm is at a position nearest to the displacement sensor as per set up (Fig. 2).

To justify the zero pressure gradient flat plate laminar boundary layer the velocity profiles are drawn at three different locations deemed critical for measurements and with no slip condition at the wall a good match with Blasius profile is met (Fig. 3). The time average velocity is calculated from 500 images on 50 points across the boundary layer thickness. A good agreement with Blasius solution confirms the zero pressure gradient (zpg) nature of the boundary layer at the given location. Secondly the turbulence intensity is found out to be 3% towards the boundary layer edge.

A. Jet Exit Velocity Profile

The vertical component of the exit velocity (velocity component downward blown away from the orifice is taken positive and vice versa) across the orifice exit are extracted from the phase averaged measurements at the given phase points pertaining to each vortical structures namely hairpins (HP), stretched vortex rings (SVR) and tilted vortex rings (TVR). The spatial-averaged velocity, $\tilde{u}_{o(t)}$ at the maximum blowing i.e. t/T = 0.25 is also obtained (dash line) across the plane at y/D_o=0. The spatial-averaged velocity is also compared with the theoretical results obtained. The positive velocity, y-component indicates blowing out of the orifice and similarly the negative velocity indicates suction into the orifice and x/D_o= +0.5, -0.5 corresponds to upstream and downstream edges of the orifice respectively (Fig. 4).

It appears that there is a sort of imprecision in the experimental measurements when compared to the theoretical values as there is a discrepancy of about 11% in the final calculated and measured values of $\tilde{u}o(t)\,|\,y/Do=0.2$. As such this uncertainty is not unanticipated as the theoretical model [6] was derived exclusively for quiescent conditions. Certainly in quiescent conditions the exit jet does not experience any additional shear from either side in the absence of any cross flow and secondly under such conditions the boundary layer remains totally absent to offer any shear from within. Secondly the uncertainty is likely to be enhanced to some extent because of the reason that the PIV measurements are taken at about 0.2Do from the wall surface. However the experimental values of $\tilde{u}o(t)$ appear to validate the theoretical model with reasonable accuracy.

TABLE I
NOMENCLATURE

Symbol	Quantity	Symbol	Quantity
D	diameter of cavity or orifice, mm	*St*	Strouhal number
		δ	boundary layer thickness
f	diaphragm oscillation frequency, Hz	*U*	characteristic velocity, m/s
		VR	velocity ratio
L	dimensionless stroke length	*x*	streamwise distance, mm
Re_L	Reynolds number based on dimensionless stroke length	y	normal distance from wall
		z	spanwise distance, mm
R_θ	Reynolds number based on momentum thickness	Subscripts	
		c	cavity value
		o	orifice value
		∞	freestream value

TABLE II
CASE SUMMARY FOR PIV TEST

Vortex	f	Δ	V	S	L	R_{eL}
HP	2	0.10	0.17	17	1.7	145
SVR	2	0.16	0.27	17	2.7	370
TVR	4	0.16	0.54	26	2.7	740

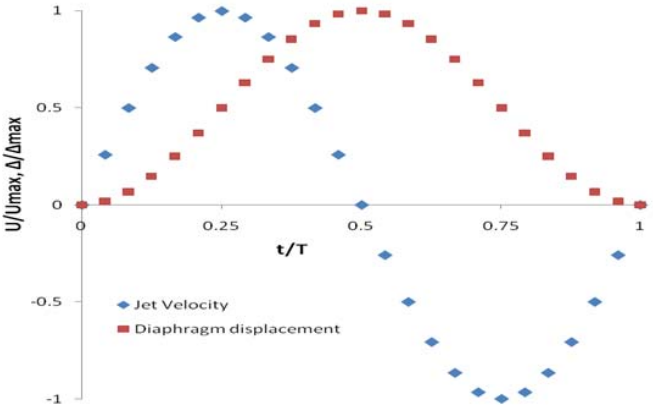

Fig. 2 Jet exit velocity and diaphragm relative position

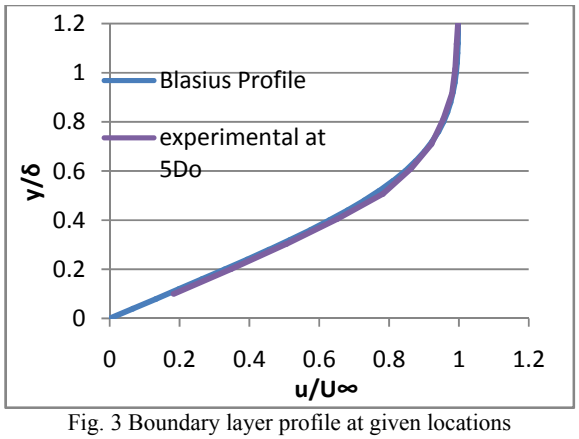

Fig. 3 Boundary layer profile at given locations

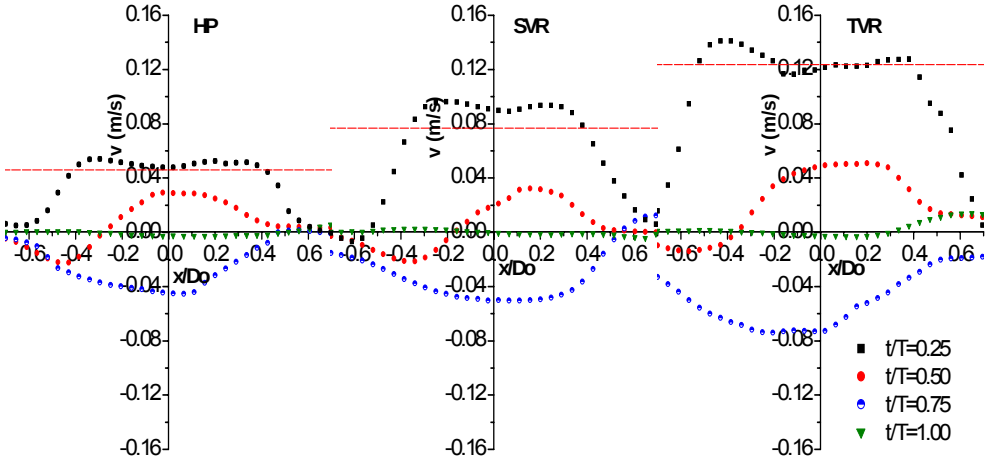

Fig. 4 Phase-averaged velocity profiles of vortical structures

B. Hairpin Vortices

The phase average measurements are taken at 4 phases equally spaced across the actuation cycle, hence giving a temporal resolution of 90°. Based on the tests carried out to check the sensitivity of number of images for reasonable quality results, phase-average flow field are obtained by recording and averaging 500 instantaneous image pairs. In figure 5 the anticlockwise vorticity indicated by red color is taken positive and clockwise is taken negative shown by the blue color. The flow direction is from left to right and the overlay of velocity vectors has also been shown. The orifice position is specified by the location 'x/Do = 0' and the measurement has been extended to the upstream point of x/Do=-1.

At t/T = 0.17 the vortex formation reveal at the earliest phase. During the complete blowing stroke both upstream and downstream branches grow up in strength although the later remains far stronger than the former. The clockwise rotation of upstream branch is weakened by the presence of resident vorticity having opposite sense. From the very first appearance when the feeble upstream branch is at its very initial forming stage it has to encounter relatively stronger resident vorticity in the opposite sense and therefore remains the main reason to weakening during the blowing stroke. Actually the blowing stroke of the cycle meant to the period during which both the upstream and downstream branches are to grow in full strength before the suction stroke begins immediately after t/T = 0.50. As such this is true to both branches but due the opposite sense of resident vorticity the upstream branch weakens a great deal. At t/T = 67, the suction stroke has had begun and the structure eventually detaches and moves away from the wall surface under the influence of self induced velocity. As the suction stroke begins the vorticity of the upstream branch has had to suffer, in that the ambient fluid is started to be sucked back into the orifice as can be seen clearly from the velocity arrow direction. However, the suction fluid does not affect the downstream branch a great deal as such since at the start of the stroke it has had moved sufficiently away from the orifice under the influence of self induced velocity. Thus the suction of the ambient fluid further results in the weakening of the upstream branch and it can be seen at t/T = 0.67 the upstream branch succumbs and vanishes completely as it could not sustain the effect of suction. Hence the birth of hairpin vortex becomes inevitable that is a vortex without the upstream branch. Though as evident from the plan view of dye visualization results [4], two counter rotating vortex legs remain significantly symmetric. As the upstream branch moves away from the orifice the suction fluid is blocked considerably although eventually it is sucked back during the remaining stroke. Hence the sucked-in fluid from both upstream and downstream sides of the orifice remains sort of disproportionate.

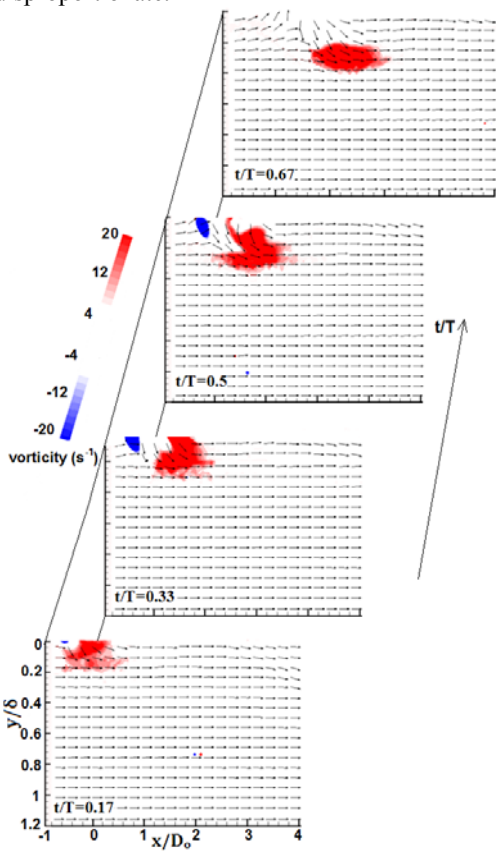

Fig. 5 Phase-average vorticity contours for hairpins

C. Tilted Vortex Rings

The sequence of evolution of tilted vortex rings is shown in Fig. 6 with an overlay of uniformly distributed velocity vectors. The formation of newer structure can be seen at t/T = 0.17 where the downstream branch is more prominent than the upstream counterpart and both the branches gain strength as the blowing stroke goes on and gain peak potency at t/T = 50. As the vortical structure moves away from the wall it remains attached with the wall by virtue of the trailing fluid column owning to the fact that a larger volume of fluid is expelled from the orifice compared to hairpins.

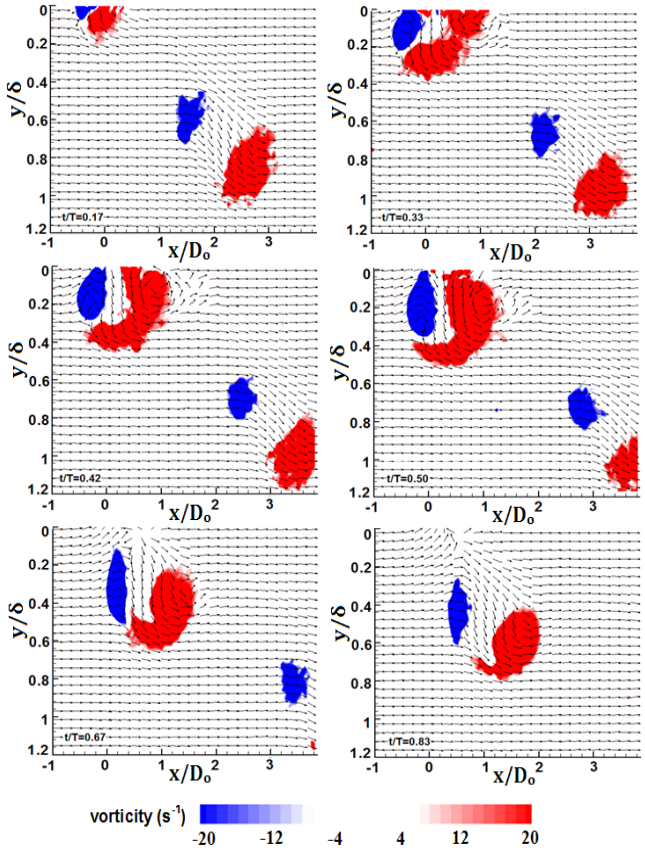

Fig. 6 Phase-averaged vorticity contours for TVR

Unlike hairpins the upstream branch remains fairly strong and the effect of resident vorticity is rather subdued. Since the resident vorticity opposes the clockwise rotation of the upstream branch and fortify the downstream branch, therefore the downstream branch appears to be more dominant. However both the branches are far stronger with more intense rotational vorticity owning to the fact that they are formed at larger value of Re_L. Secondly such an intensified vorticity can also be tracked back to the jet exit velocity profile where it was shown that the higher jet exit velocity profile with more top-hat like shape suggests a greater roll up in the vortex core. The strength of the upstream branch remains comparable to that of the downstream branch owning to the fact that such structures are produced at larger value of VR. As a result the tilted vortex ring exhibits a rather symmetric structure as a whole. An extended zone trailing behind the primary vortex can also be seen where velocity vectors appear directing towards the vortex and inclined at an angle with the wall. Such a zone is best observed at t/T = 0.17 and t/T = 0.83 behind the structures and is believed to be formed by the upwash motion of the trailing structures called secondary vortices. However one might tend to view the tilted vortices less useful to disturb the near wall fluid. Actually it is the trailing secondary and induced tertiary vortices that remain within the boundary layer and exchange momentum with the less energetic near wall fluid making such structures the most effectual in terms of flow separation control effect.

IV. Summary and Conclusion

The operational parameters of SJA are varied at will while keeping the geometrical parameters same to produce vortical structures in the boundary layer and three different type of such structures are indentified namely hairpin vortices, stretched vortices and tilted vortex rings. In essence the stretched vortices are the in between form of hairpins and TVR's and therefore behave more like hairpins in that they undergo similar stream wise stretching under the influence of boundary layer shear, so the reason to not discussing them in detail in this work. When the SJA is operated at relatively large value of 'VR' and 'L' the tilted vortices are produced which are demonstrated by the more recent quantitative studies the most desirable structures considered towards flow separation control. The streamwise secondary and trailing tertiary vortices trailing behind the tilted vortex rings behave in the similar manner as the long-stretched typical hairpin legs in terms of transferring the high momentum fluid from the outer region of the boundary layer to replace the relatively less energetic fluid near the wall surface.

Acknowledgment

The first author would like to thank University of Engineering and Technology Lahore, Pakistan to fund his PhD studies and thanks are due to Dr. S. Zhang for his valuable assistance to build the rig for the experimental work.

References

[1] Acarlar, M.S. and Smith, C. R.; A study of hairpin vortices in a laminar boundary layer, Part 2. Hairpin vortices generated by fluid injection; Journal of Fluid Mechanics, Vol. 175, 1987.
[2] Glezer, A.; The formation of vortex rings; Phy. of Fluids, V. 31,9, 1988.
[3] Guo, F and Zhong, S.; A PIV investigation of the characteristics of micro-scale synthetic jets; The Aer. Journal, l. 111, No. 1122, 2007.
[4] Ishtiaq A. Chaudhry, Shan Zhong: Understanding the interaction of synthetic jet with the flat plate boundary layer; ICARME, Trivandrum, India, May 2012.
[5] Jabbal, M. and Zhong, S.: The near wall effect of synthetic jets in a boundary layer; Int. J. of Heat and Fluid Flow, V 29, issue 1, 2008.
[6] Tang, H; Performance modelling of synthetic jet actuators for flow separation control; PhD thesis, School of Mechanical, Aerospace and Civil Engineering, University of Manchester, UK, 2006.
[7] Zhou, J. Zhong, S. "Coherent structures produced by the interaction between synthetic jets and a laminar boundary layer and their surface shear stress patterns". Computers and Fluids. Vol. 39. Issue 8. 2010.